geosciences

MDPI

Article

# Classification of Red-Bed Rock Mass Structures and Slope Failure Modes in South China

**Cuiying Zhou, Xu Yang, Yanhao Liang, Zichun Du, Zhen Liu *, Wei Huang and Weihua Ming**

Guangdong Engineering Research Centre for Major Infrastructure Safety, Sun Yat-sen University, Guangzhou 510275, China; zhoucy@mail.sysu.edu.cn (C.Z.); yangxu9@mail.sysu.edu.cn (X.Y.); liangyh33@mail2.sysu.edu.cn (Y.L.); duzichun@mail2.sysu.edu.cn (Z.D.); huangw226@mail2.sysu.edu.cn (W.H.); mingwh@mail2.sysu.edu.cn (W.M.)

* Correspondence: liuzh8@mail.sysu.edu.cn

Received: 30 January 2019; Accepted: 17 June 2019; Published: 21 June 2019

check for updates

**Abstract:** Red beds are Meso–Cenozoic continental sedimentary strata that are mainly composed of gravel stone, sandstone, siltstone, mudstone, and shale and occasionally have interlayers of limestone, halite, and gypsum. As a typical rock mass, red beds are widely distributed throughout South China. In a typical tropical and subtropical continental environment, red beds are the product of multiple sedimentary cycles, which have resulted in complicated rock mass structures that play an important role in rock mass stability. It is thus of great significance to investigate the influence of different rock mass structures on the stability of red-bed slopes. In this paper, the geological formation history of red beds in South China is described. The main features of red-bed rock mass slopes in South China are discussed. The main combinations of inner geomechanical structures comprise: (1) mega-thick soft rock structures; (2) mega-thick hard rock structures; (3) thick hard rock structures with weak intercalation; and (4) soft–hard interbedded structures. In addition, the features of slope failure are analyzed, and four common failure modes are identified from the statistical data: (a) weathering spalling and scouring; (b) rock falls; (c) landslides; and (d) tensile dumping.

**Keywords:** red beds in South China; structural plane; structural morphology; rock mass structure types; slope failure model; forming feature of hazards

## 1. Introduction

The term red beds refers to red clastic rocks weathered in laterite from the Mesozoic–Cenozoic era. They include lacustrine deposits, fluvial facies deposits, interbedded lacustrine–fluvial deposits, and piedmont diluvial deposits. Red beds primarily consist of conglomerate, sandstone, mudstone, siltstone, and shale, as well as a small amount of limestone, rock salt, and gypsum [1–5]. These beds are formed under unique hot and dry tropical–subtropical environmental conditions, and they exhibit a series of unique engineering properties, such as high porosity. We can investigate the diagenetic evolution of red beds through a petrophysical, fluid evolution, and thermal history analysis [6]. No distinct boundary exists to distinguish red-bed rock mass from conventional soil mass. In particular, the water-induced instability problem is significant for red beds. According to a previous model, the instability of red-bed soft rock slopes is mainly due to the softening that is induced by water infiltration [7,8].

Previous research has shown that red beds are widely distributed all over the world [1,9–13], including Asia, Europe, and America. In China, the exposed area of red beds is approximately 0.826 million km$^2$, which is second only to the carbonatic area, which is an estimated 0.910 million km$^2$ [1,2]. The statistics show that 80% of the red-bed area in China is distributed in a humid region that spreads from the east of the Qinghai–Tibet Plateau to the south of the Qinling and Huaihe River, and the involved red-bed area accounts for approximately 60% of the total area of the humid regions. Figure 1 shows the distribution of red-bed basins in China [1].

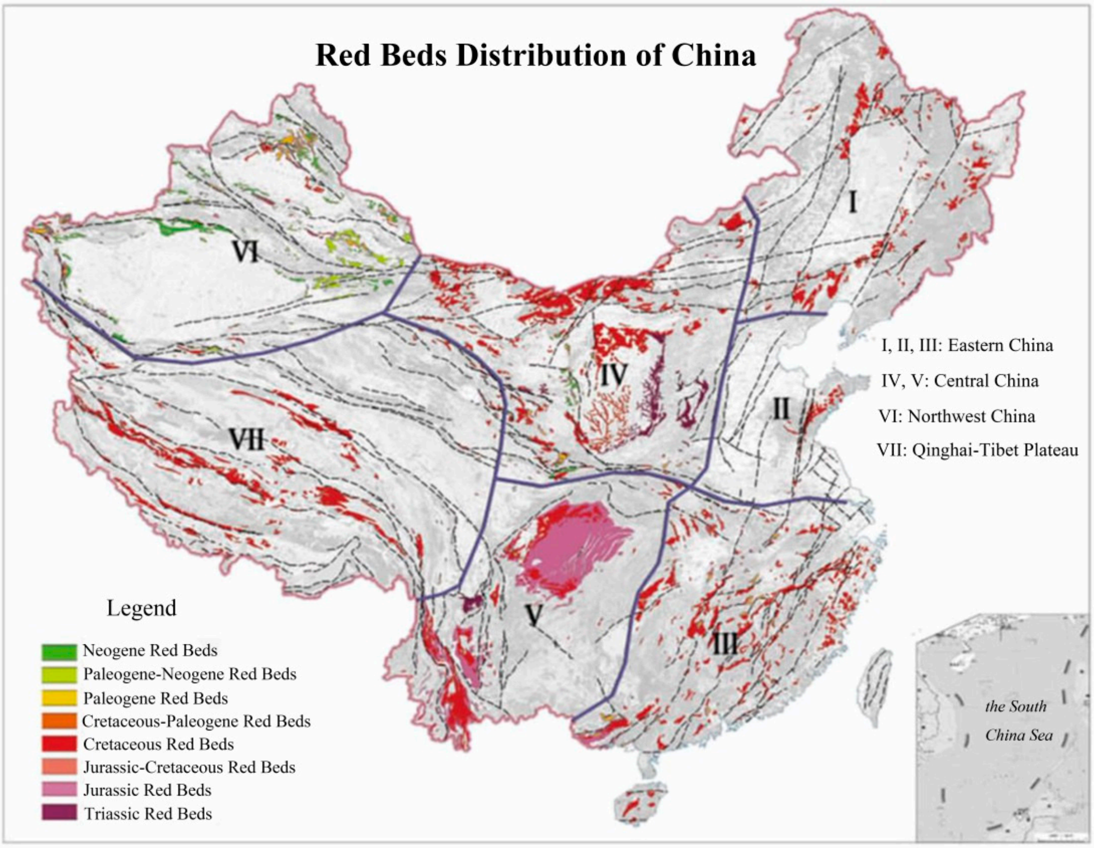


**Figure 1.** Distribution of red beds in China [1].

Red beds have undergone long-term geological formation and transformation [14–23], which have resulted in a typical sedimentary soft–hard interbedded structure of mudstone and sandy conglomerate. A weak bedding layer with a low coalescence degree but good extensibility is usually formed at the interface between the hard and soft rocks and it is one of the main structural planes observed in red beds. The strata of red-bed soft rock generally contain one or more weak interlayers. For example, sandstone contains a mudstone interlayer, which softens easily and fails when it meets water. The mechanical properties of red-bed soft rock containing weak interlayers can be studied by laboratory and field analyses of the mineralogical composition of the weak interlayer [24,25]. Structural features such as faults, joints, interlayer slippage zones, and pelletization dissection are usually well developed and are considered to be other types of main structure plane in red beds, such as the interlayer slippage zone (a structurally related feature) of red beds located in southwestern China [26] and faults or fractures at the depth of red beds in the South Georgia Rift (SGR) basin [27].

It is well known that rock mass structures play a dominant role in the stability of a rock mass [11,16,28]. The characteristics of slope failures in red beds are summarized from field investigations and case studies as follows:

(1) A progressive failure is prone to occur on a slope with structures controlled by steep dip joints and fissures. Once the initial damage occurs, sustained destruction will occur progressively.

(2) The slope of rock mass structures that are controlled by weak interlayers is prone to causing hazards. Alternatively, a rock slope with thick layers of hard rock mass may also tend to suffer from considerable serious damage if underlying weak layers exist.

(3) A slope with structures controlled by the structural plane of a composite rock mass is likely to fail, even if it is a rock slope with nearly horizontal layers.

The classification of rock mass structures is useful for the stability analysis of slopes, tunnels, or foundation pits in red-bed areas. In addition, the examination of the structures of a red-bed rock mass is essential for investigating the characteristics of structural planes, such as internal bedding planes, joints, cracks, and weak interlayers. In addition, it is important to investigate the concurrent action of structural planes and structural morphologies. Many researchers have been studying the classification of rock mass structures in red-bed slopes by concentrating on factors such as the distribution characteristics (fractal character, crack width, intensive degree, etc.) of the structural plane, the intersection angle of the structural plane relative to the slope, and the integrality and strength of the rock mass [19,29–31]. The strength, stiffness, and dip angle of the rock mass structural plane directly influence failure modes [32,33]. The key structural plane can effectively reveal the nature of rock slope stability and provide a dimensional discriminant approach for studying the stability of the rock mass slope [34].

However, the current classification of red-bed rock structures has mainly been based on the red beds in Sichuan and Hunan provinces in China. To the best of our knowledge, no extensive studies have been carried out with respect to the red beds in South China regions, such as Guangdong and Guangxi provinces. The red beds in these regions exhibit special regional characteristics due to abundant rainfall and intense engineering activities, which might cause more disastrous slope failures. Thus, there is high value in carrying out an extensive investigation to classify red-bed rock mass structures in South China.

In this study, a classification of the red-bed rock structures in South China was conducted, and the main failure modes of the red-bed slopes were identified on the basis of an extensive analysis of red beds in the north of Guangdong Province. The results were obtained by analyzing more than 10 highway projects using on-site measurement, remote sensing, drilling, and geological survey. This study can provide reference values for intended large-scale projects in the red-bed distribution area of south China.

## 2. Geological Background of Red-Bed Formation in South China

Because of the unique hot and dry tropical–subtropical formation environment, the red-bed rock layer is rich in $Fe_2O_3$, which gives the rock mass its red color [1]. From the perspective of the formation and evolution history of the geological conditions in South China, the red beds in this area possess the following four major characteristics:

(1) The red-bed distribution in South China is affected by the main fault zones. The fault zones (mainly oriented northeast (NE) and north-northeast (NNE) in South China) are deformations along the Cathaysian–New Cathaysian tectonic system [15,35]. The red beds in South China are scattered along these fault zones. Figure 2 shows the distribution of red-bed basins and major fault zones in Guangdong Province in South China.

(2) Four topographic features are present from the edge to the center of the red-bed basin in South China [1]:

I. A basin surrounded by mountains, which specifically refers to a red-bed basin surrounded by mountainous areas and faults that bound the basin.
II. Danxia landform, in which several vertical structural planes are well developed, cutting the rock bed into columnar or platelike structures.
III. Red-bed hill zone, which refers to hills with moderate slopes that are made of rock beds consisting of sandstone or shale.
IV. Center plain zone [1], which refers to the central part of a red-bed basin. This zone is generally formed by the sedimentation of fine-grained clastic lacustrine facies and alluvial flat facies. The lamellar-structured red beds were formed with small dip angles and were slightly influenced by tectonic movement.

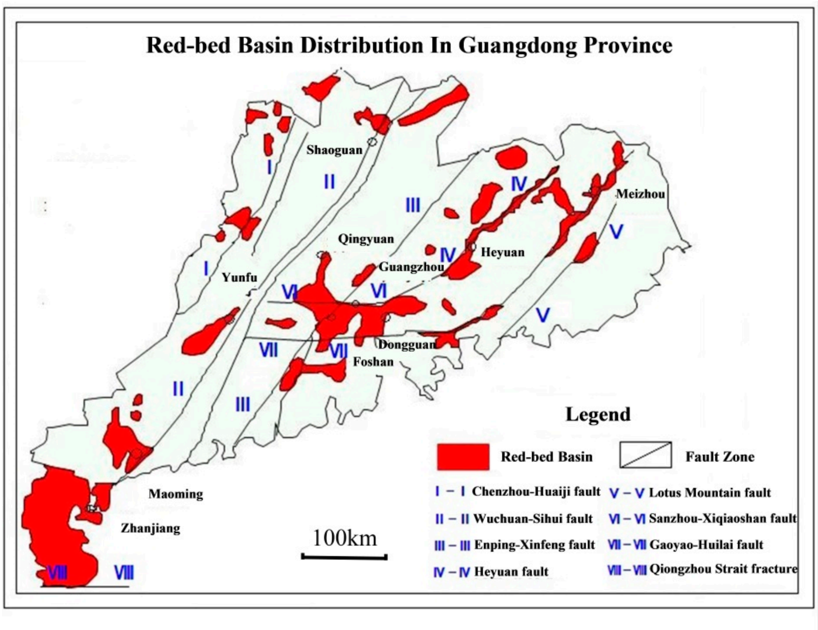


**Figure 2.** Distribution of red-bed basins and principal fault zones in Guangdong Province [1].

(3) The particle size distribution and the attitude of the stratum are closely related to the sedimentation process. The red-bed sedimentation materials mainly originate from the ancient basin and the efflorescence of rocks, so thick glutenite emerges at the edge of the red-bed basin with the sedimentation of large particles, the size distribution of which is consistent with that in the fracture zone at the edge of the basin. Fine particles are transported to the center of the basin during the sedimentation process. From the edge to the inner zone of the basin, the size of sedimentary particles gradually decreases, and the rock bed becomes thinner, as shown in Figure 3. In addition, as a result of the influence of local sedimentation, rock beds in South China usually tend to be interbedded without uniform thickness. The adhesion force between neighboring rock beds is weak, and the axial planes of gentle undulating folds usually have dip angles of more than 60° [15] (see Figure 4).

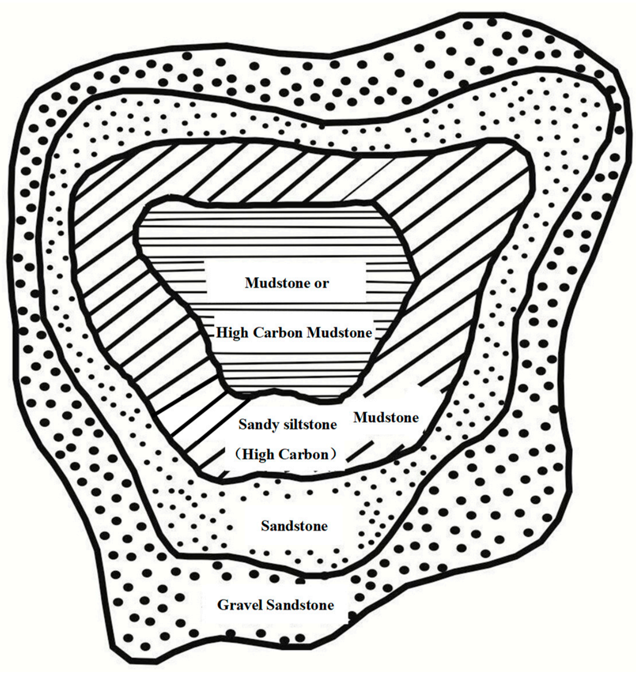


**Figure 3.** Typical red-bed sedimentary model in South China.

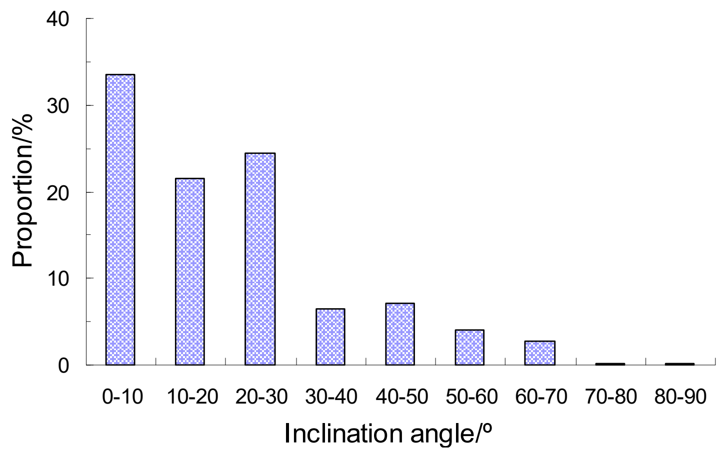


**Figure 4.** Statistics of the red-bed inclination angle of bedding attitude in South China.

(4) The quaternary cover, consisting mainly of the red-bed weathering products and quaternary-impacted proluvium with high laterization, can be easily found in red-bed areas in South China. The soil in the cover tends to have poor engineering properties.

## 3. Inner Structures of Red Beds in South China

The survey area is the key distribution area of red beds in Guangdong province, and the Danxia landform has been declared a world natural heritage. At the same time, the survey area is also crossed by many expressways. Geological exploration is mainly carried out by means of remote sensing, in situ monitoring, and referencing geological surveys. The structural planes and their features in South China were classified by investigating the exploration data (including over 10 expressways) of red beds in the north of Guangdong Province.

(1) Primary stratification

The red beds in South China demonstrate a distinct bedding structure with a low degree of coalescence, as shown in Figure 5a. This bedding can be stripped off naturally after weathering. Most fresh bedding has a monoclinic attitude and dip angles in the range of 0–30°, as shown in Figure 4. The dip angles of some local rock masses may vary considerably because of tectonic movements, but they are generally still below 50°.

(2) Secondary stratification

Complicated faults develop as a result of strong geological structure activity. There are more than 1000 large-scale fractures in Guangdong province, among which 26 are deep (most are in sial and sima) and large (over hundreds of kilometers in length) in the NE and NNE directions [1]. Structural activities cause the fractures to slide along the soft–hard interface and primary weak interlayer in the red beds, contributing to the formation of bedding fault zones and even shattered zones, namely, the weak interlayer reworked by tectonism.

As a result of the long-term influence of underground water and continuous wet–dry cycling, pelletization phenomena can be observed, and mudded intercalation is thus formed. The thickness of most weak interlayers ranges from 2 to 9 cm, and some of them can be 10–18 cm. The distribution density is 1–4 layers per meter and can locally reach 7–10 layers per meter. The primary stratification near the faulted and cataclastic zones usually has a larger density (15–20 layers per meter). In addition, the joints of the red beds in South China tend to have a high distribution density, and their intersection angles are mainly vertical, which decreases the continuity and strength while increasing the degree of anisotropy of the rock mass. Weathering fissures are usually developed on the surface with dip angles that range between 70 and 90°. Both weathering fissures and main bedding distribution are shown in Figure 6.


(**a**) Primary stratification (substance differentiation stratification)

(**b**) Secondary stratification made by clay intercalations

**Figure 5.** Two typical structural stratifications of red beds in South China.

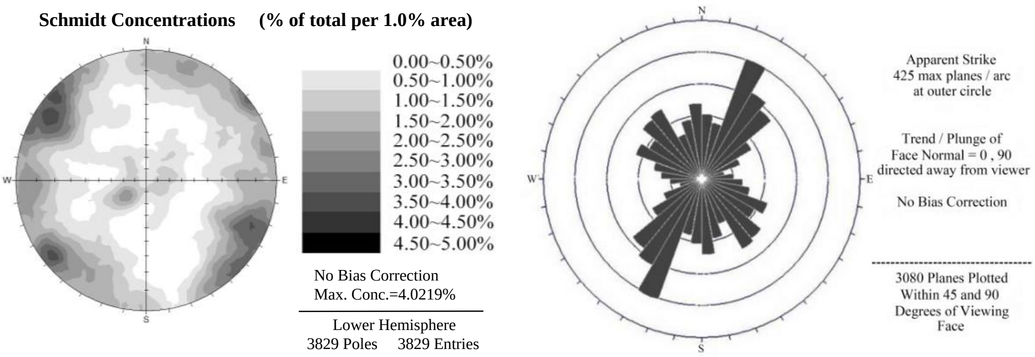


(**a**) Weathering fissures

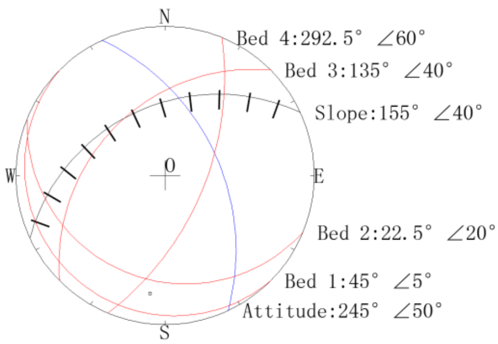


(**b**) The main bedding

**Figure 6.** Average distribution of red-bed superficial weathering fissures and main bedding in northern Guangdong province in South China.

In addition to interbedded stratifications, steep-inclined stratifications also develop from the top to the bottom of many red beds' slopes in South China. According to statistical analysis, between two and four groups of bedding planes with a spacing of 70–90 cm develop in most red beds. The lengths of these bedding planes are not uniform and mainly range from 10 to 50 cm. The proportion of bedding planes with spacings of less than 90 cm is approximately 90%, as indicated in Figure 7. This type of bedding plane is commonly observed in the hard rock mass at the fringe of red-bed basins, which can extend from several meters to dozens of meters, cutting the rock mass into columnar or platelike pieces.

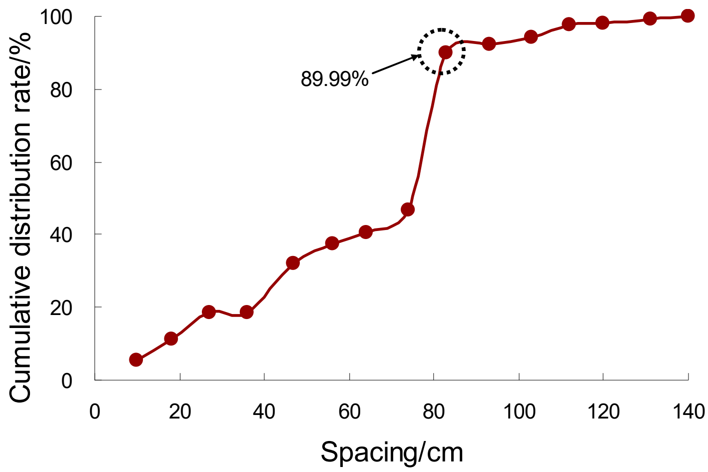


**Figure 7.** Cumulative distribution curve of the steep structural face spacing of red-beds' slopes in South China.

### *3.1. Red-Bed Litho-Structural Facies in South China*

According to the field investigation and data analysis, three rock mass facies of red beds were identified.

(1) Mega-thick stratum

Mega-thick stratum includes mega-thick (>150 cm) hard rock and mega-thick soft rock. In the former glutenite predominates, while the latter is mainly composed of mudstone, silty mudstone, and argillaceous siltstone, as well as intensively and fully weathered glutenite layers. This combination of lithologies can be easily found at the edge of the red-bed basins. In this type of lithology, weathering and erosion occur along vertical joints in the multiple mega-thick stratums. The Danxia landform formed gradually and it tends to collapse in the red-bed distribution areas. Danxia landforms are sedimentary red clastic rocks deposited in intermountain basins in Neogene, which formed through the dynamic action of tectonic movement [36,37]. The rock mass with this structural condition is assumed to be affected by water and have weak engineering properties and usually suffers from sliding failures.

(2) Soft–hard interbedding of sandstones and mudstones

These facies are commonly observed in the center of red-bed basins. Particles constituting sandy stones are usually coarse. Sandstones have high strength (compressive strength of about 30 MPa) and good permeability (permeability coefficient of about $1 \times 10^{-2}$ cm/s), whereas mud shale is generally fine and very weak (compressive strength <20 MPa) with low permeability (permeability coefficient of about $1 \times 10^{-4}$ cm/s). Hence, this type of litho-structural facies tends to soften in water. Slopes containing this type of lithology are likely to undergo sliding failures along the weak mud shale layers. In particular, slopes made of soft–hard interbedding of sandstone and mudstone can cause sliding failures [38,39].

(3) Mega-thick hard rock with soft–hard interlayers below or thick hard rocks at the top and bottom with soft–weak intercalated layers in between.

These facies are observed at the transitional zone between the edge and the center of red-bed basins. Soft–weak interbedded layers are influenced by underground water and rainfall and experience wet–dry cycling. Thus, there also exists a notable pelletization phenomenon, and mudded intercalation has weak mechanical properties.

### 3.2. Structural Types of Rock Mass in Red Beds in South China

As analyzed in the above sections, dip angles of rock mass in red beds in South China range mainly from 0 to 30°. According to the intersecting angle formed between the rock strata and the slope surface, the rock mass structures can be divided into nearly horizontal/slightly inclined structures (angles from −15 to 15°) [30,40] and inclined structures (angles from 15 to 50°) [19]. Inclined rock mass structures can be further divided into consequent layered inclined structures and anti-dip layered inclined structures. Steep or vertical slope structures are seldom seen in red beds in South China. Considering the different litho-facies and anisotropies (e.g., joints, fractures, and soft–weak interlayers), the rock mass structures in South China are further categorized as shown in Table 1.

## 4. Results and Discussion

### 4.1. Disastrous Characteristics and Failure Mode of Red-Bed Slopes in South China

The red beds in South China are the result of a long geological process. Most of them possess soft–hard interbedded internal structures due to the alternate sedimentation of mudstone. The folds and faults zones are well developed. Meanwhile, the original weak bedded planes and interlayers, which significantly influence the stability of slopes, experienced wet–dry cycling and substantial pelletization induced by rainfall and underground water. Because of rainfall and human activities, geological hazards (e.g., weathering, slope scouring, slumping, and landslides) have become notable. According to the statistics [41], the occurrence probability of weathering in the red-bed slopes in South China is approximately 100%. In addition, slumping, landslides, and tensile cleft dumping, as shown in Figure 8, account for 68.37%, 23.26%, and 8.37%, respectively, of all geological hazards in the red beds [41].

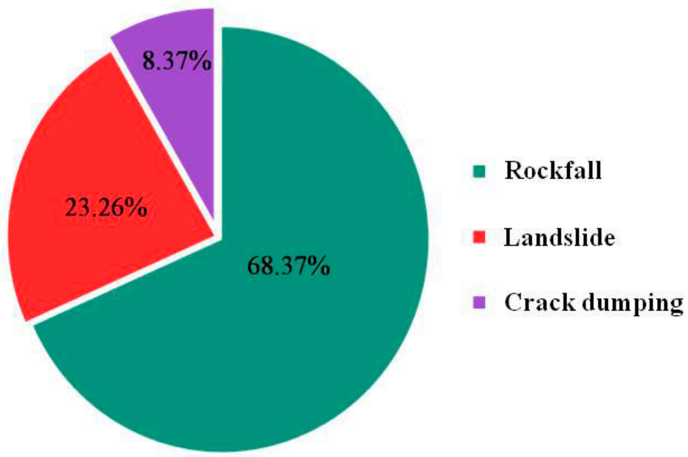


**Figure 8.** Proportion of geological hazards in red-bed slopes in South China.

**Table 1.** Rock mass structure of red-bed slopes in South China.

| The Type and Class of Rock Mass Structure | | Structural Feature | Engineering Geological Evaluation | Rock Mass Structure Diagram |
|---|---|---|---|---|
| Thick-layered hard rock mass structure | Global-layered | Complete rock mass consisting of mega-thick glutenite with a layer spacing of more than 150 cm; no more than one set of orthogonal steep dip joints developed in the inner zone | Hard and locally uniform structure with primary closure joints in majority; mega-block is the structural morphology with good stability but prone to local collapse and slide | 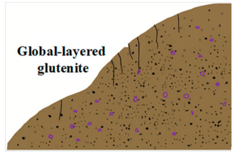  |
| | Block-layered | Relatively complete rock mass consisting of thick-layered glutenite with a layer spacing of between 100 and 150 cm; structural plane developed with a spacing of between 80 and 100 cm | Relatively hard structure with a block or cylinder as the main structural morphology; relatively stable with cracks developed along the structural plane; prone to collapse and slide | 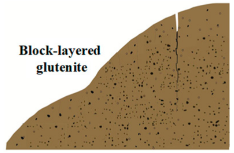  |
| Thick-layered soft–weak rock mass structure | | Composed of thick-layered soft–weak rock mass deposits or consists of thick layers of intensively weathered conglomerates (more than 20 m in thickness) | Relatively weak slope; developed structural plane; rock thickness of 0.5 to 15 m; prone to collapse and slide | 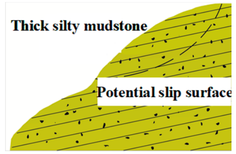  |
| Thick-layered hard rock mass structure with soft–weak rock mass | With soft–weak interlayer (including clayey layer) | Hard rock mass, such as thick-layered glutenite, with a thin-layered weak clayey rock mass, which includes a clayey layer of soft–weak rock mass formed by the wet–dry cycling and weathering | The upper hard rock mass can easily slide horizontally along the plane of the soft–weak rock mass or collapse to a free face | 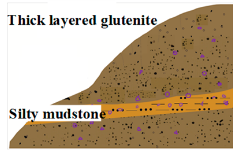  |
| | With soft–hard interbedded rock mass | Mega-thick-layered or thick-layered hard rock mass with a soft–hard interbedded rock mass below, such as sand mud and sand shale | The upper hard rock mass can easily slide horizontally along the plane of the soft–weak rock mass or collapse to a free face | 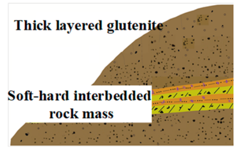  |
| Soft–hard interbedded rock mass structure | | Soft–hard interbedded rock mass with different thicknesses with a layer spacing ranging from 10 to 50 cm; developed structural planes with thicknesses ranging from 2 to 9 cm and a density of 2–7 per meter (15–20 per meter in some local parts) | The density of the structural planes near the fault fracture zone is the highest; easily prone to a cutting landslide | 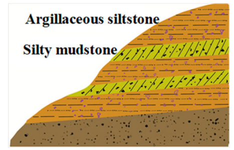  |

#### 4.1.1. Weathering and Slope Scouring

Weathering and scouring are the most common predisposing factors of slope failure in the red beds in South China. As a result of abundant and frequent rainfalls, the rocks in red-bed slopes, especially clayey rocks, undergo wet–dry cycles; the rocks gradually soften and eventually become loose rock blocks or laterite. Additionally, this process may easily lead to the occurrence of disintegration and spalling, as depicted in Figure 9.

**Figure 9.** Weathering and surface erosion in a red-bed rock slope in South China.

The weathering and scouring of red-bed slopes at a small scale are usually not easily observed. As time goes on, red-bed slopes may suffer from serious erosion, and a large number of weathering fractures may appear, which could potentially lead to large-scale (over millions of cubic meters with an exposed slope of $1 \times 10^6$ m$^2$) slope collapses [42–45]. As suggested by statistics, the volume of rock blocks as a result of weathering and scouring can reach 7 million m$^3$ with an exposed slope of $1 \times 10^6$ m$^2$ [46]. The rocks in an exposed red-bed slope are expected to transform into laterite [47].

(2) Failure mode

Previous studies have shown that under certain climatic and geological conditions, the weathering of slopes in red-bed areas in South China is mainly induced by temperature and moisture [47], especially during hot summers, during which heavy rainfalls frequently occur in South China. Fractures induced by thermal stress continue to grow and aggregate on the outer surface of red-bed slopes, causing the clastic spalling of the slope surface being affected by weathering and rain wash and contributing to the loss of soil and water. Typical slope scouring erosion along expressway A in Guangdong province is shown in Figure 10. With the loss of rock and soil mass from the outer surface of the slope, the inner part of the slope is gradually exposed to repeated weathering, which weakens the slope stability. Notably, weathered and washed loose deposits with a high degree of laterization may finally become the source materials for debris flows [48,49]. As shown in Table 1, mudstone, shale, silty mudstone, and other clay rocks on the slope of a soft–hard interbedded structure are easily scoured and soften in the presence of water.

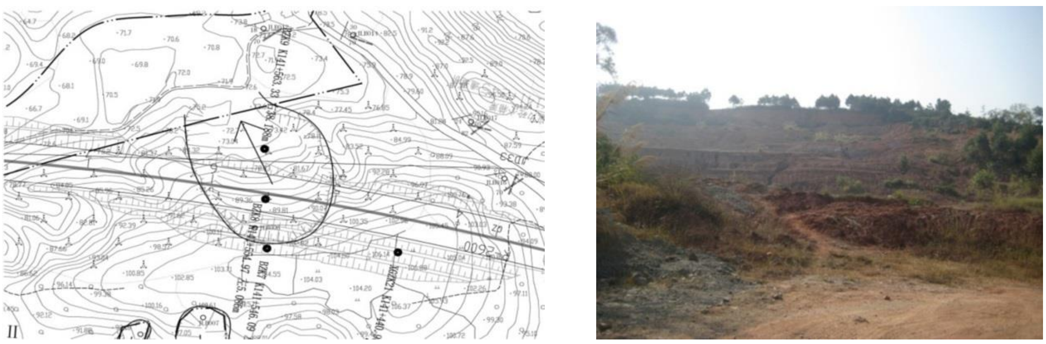

(**a**) Site location (**b**) Slope scouring erosion

**Figure 10.** Slope scouring erosion of a slope in the expressway A, Guangdong, China.

#### 4.1.2. Rock Falls

The occurrence of rock falls in a typical red-bed rock slope in South China is shown in Figure 11.

**Figure 11.** Collapse and falling in a red-bed rock slope in South China.

Rock falls are the most common geological hazards in the red beds in South China. These hazards usually take place in an area of a slope with a thick layer of glutenite, in which joint fissures are densely distributed (shown in Table 1). Rock falls also occur on slopes containing soft–hard intercalated structures and thick weak rock blocks. Slopes with soft–hard intercalated structures can collapse because of the loss of support from hard rocks, which arises from the pelletization effect as well as the serious loss of soil and water under wet–dry cycling conditions. The collapse of slopes with thick weak rock blocks is induced by the high connectivity of weathered fractures, which leads to tension cracks.

According to statistics, failures of red-bed slopes in the form of rock falls occur mostly at a small-to-medium-sized level. Small-scale collapses account for over 70%, with a volume of collapsed materials of 10–500 $m^3$, while medium-sized collapses account for approximately 30%, with a volume of collapsed materials of 800–5000 $m^3$ [50].

(2) Failure mode

Two sets of conjugate fractures usually develop in slopes with hard rock blocks (e.g., thick sandy conglomerates) in South China. With a fracture that is parallel to the slope surface, the rock mass on top of the slip surface can eventually slip under gravity, causing tension failure of other fractures and contributing to the collapse of rock blocks.

The collapse scale is mainly controlled by the cutting density and connectivity degree of the structural planes. Medium-sized collapsing occurs in large rock blocks of low cutting density and good connectivity, while in rocks of high cutting density, small-sized collapsing occurs with the generation of small broken rocks. According to thick-layered soft–weak rock mass structure and soft–hard interbedded rock mass structure described in Table 1, the collapse of thick weak rock slopes occurs because the rock mass in the superficial zone becomes loose from the effect of weathering and rain wash and thus collapses under gravity. The clayey rock mass in slopes with soft–hard intercalated structures (e.g., mudstone, shale, and powder sandy mudstone) tends to undergo geomechanical degradation and is rapidly laterized [20–22]. Long-term rain wash and serious soil erosion due to rainfall can give rise to the loss of support for the hard rock mass (sandstone and conglomerate) at the top of rock slopes, which will then lead to a small-to-medium-scale collapse (from hundreds to thousands of cubic meters).

#### 4.1.3. Landslide

Landslides account for only 23.76% of the hazards that take place in the red beds in South China and they are mostly deep (about 5–20 m) sliding failures [51]. The induced damage is generally more serious than that caused by shallow weathering and spalling, scouring, and collapsing. Figures 12 and 13 describe a landslide occurring on expressways B and C in Guangdong Province.

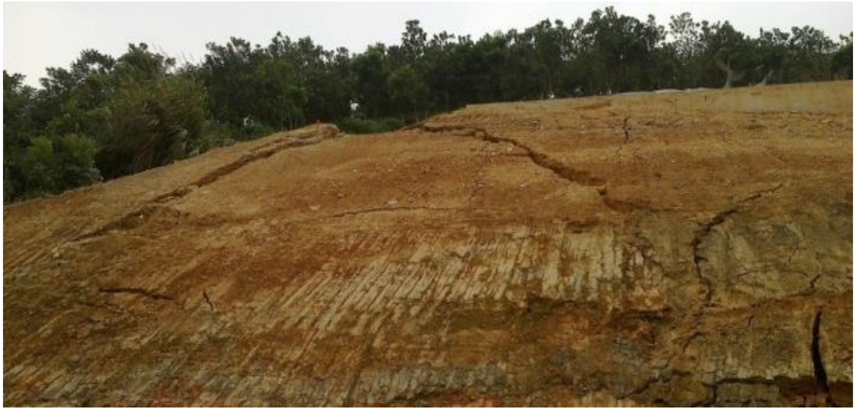

**Figure 12.** Landslide failure of a slope on expressway B, Guangdong, China.

**Figure 13.** Landslide failure of a slope on expressway C, Guangdong, China.

Landslides in the red beds in South China are closely related to rainfall [52]. In general, glutenite has a high permeability, while the permeability of shale is relatively low in glutenite–mudstone interbedded layered structures (thick-layered hard rock mass structure with soft–weak rock mass in Table 1). In rainy weather, perched water is mainly generated at the sand–mud interface, causing an increase in pore-water pressure. In addition, periodic wet–dry cycling leads to pelletization in the weak intercalated layers and interlayer fracture zones. Sliding failure occurs along the weak structural plane in the bedding slopes as well as the reverse pour slopes.

We investigated the red-bed and slope engineering in northern Guangdong, which has the typical red-bed distribution area of South China. The specific research area is shown in Figure 14a, and its contour map is shown in Figure 14b.

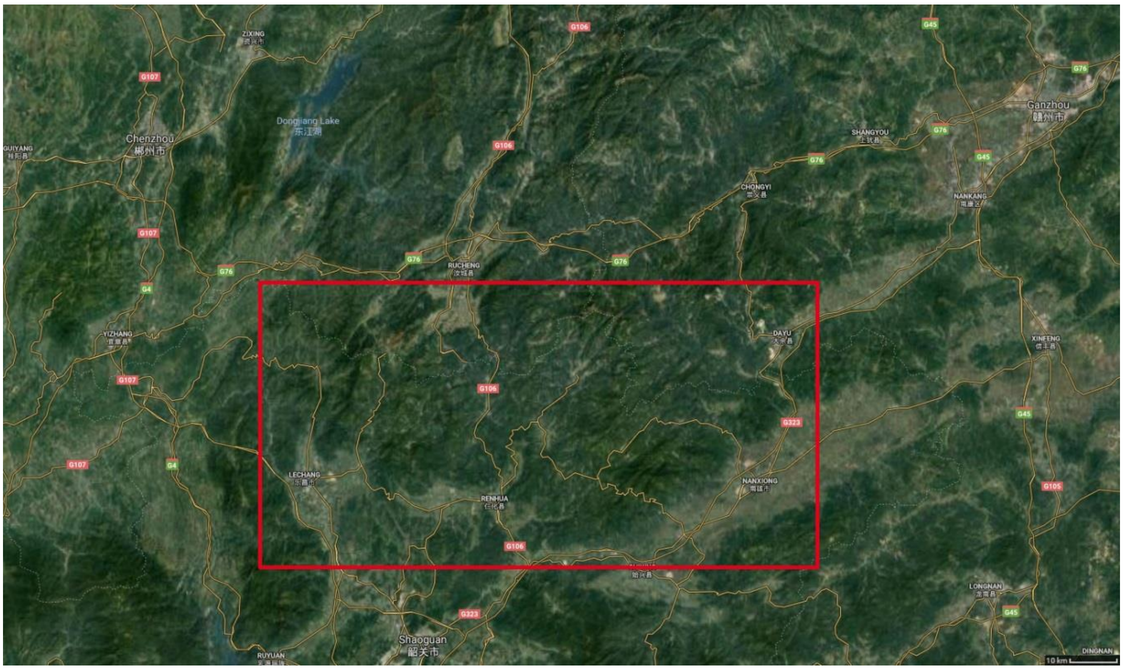


(**a**) Research area

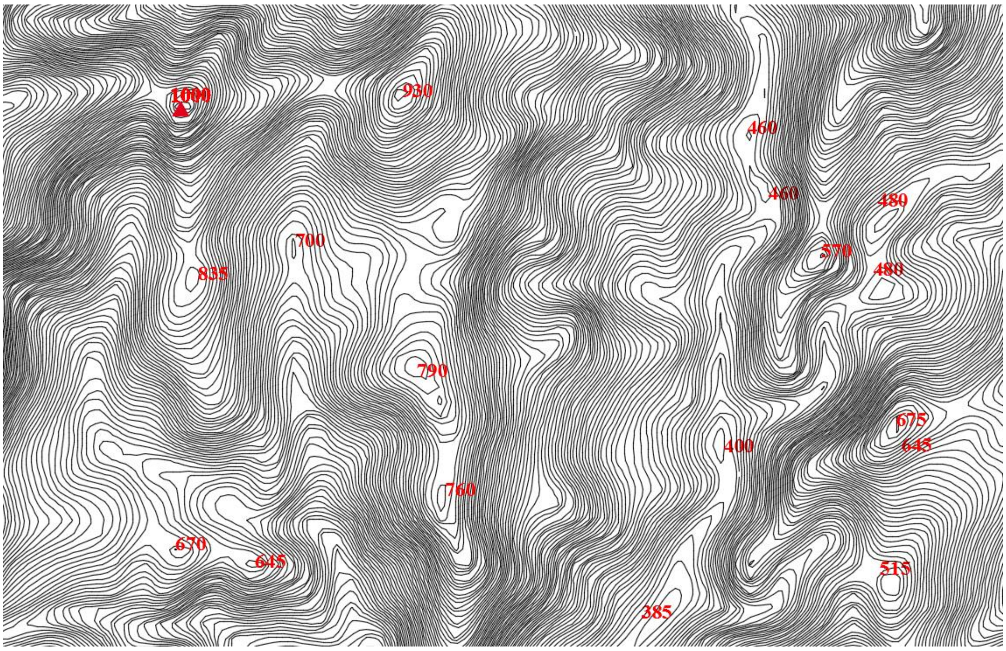


(**b**) Contour map (precision is 5 meters)

**Figure 14.** Major research areas in northern Guangdong province.

The daily rainfall data of Guangdong Meteorological Bureau were used to determine daily rainfall discharge in Heyuan, Meizhou, Qingyuan, and Shaoguan where the red-bed soft rock mainly distributes. In Figure 15, it can be seen that the rainfall in these areas is abundant and mainly concentrated in the period between February and September, of which February–March is the plum rain season, April–June is the monsoon rainy season, and July–September is the typhoon rainy season. Long-term abundant rainfall is the main cause of slope weathering and landslides in the research area.

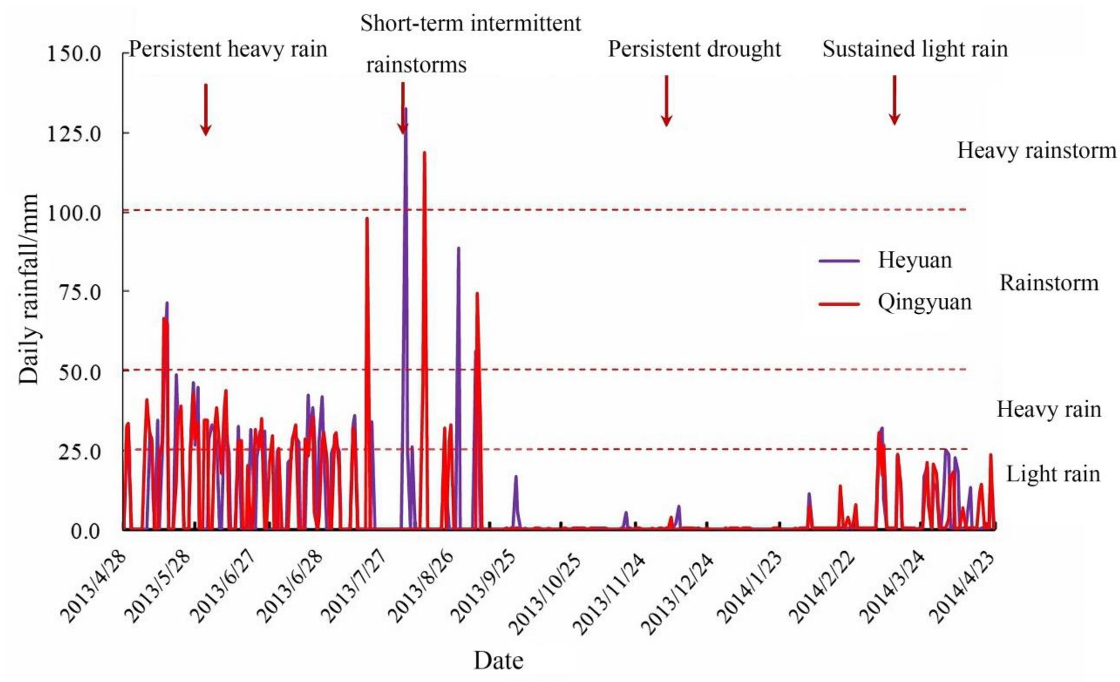


(**a**) Daily rainfall distribution map of Qingyuan-Heyuan

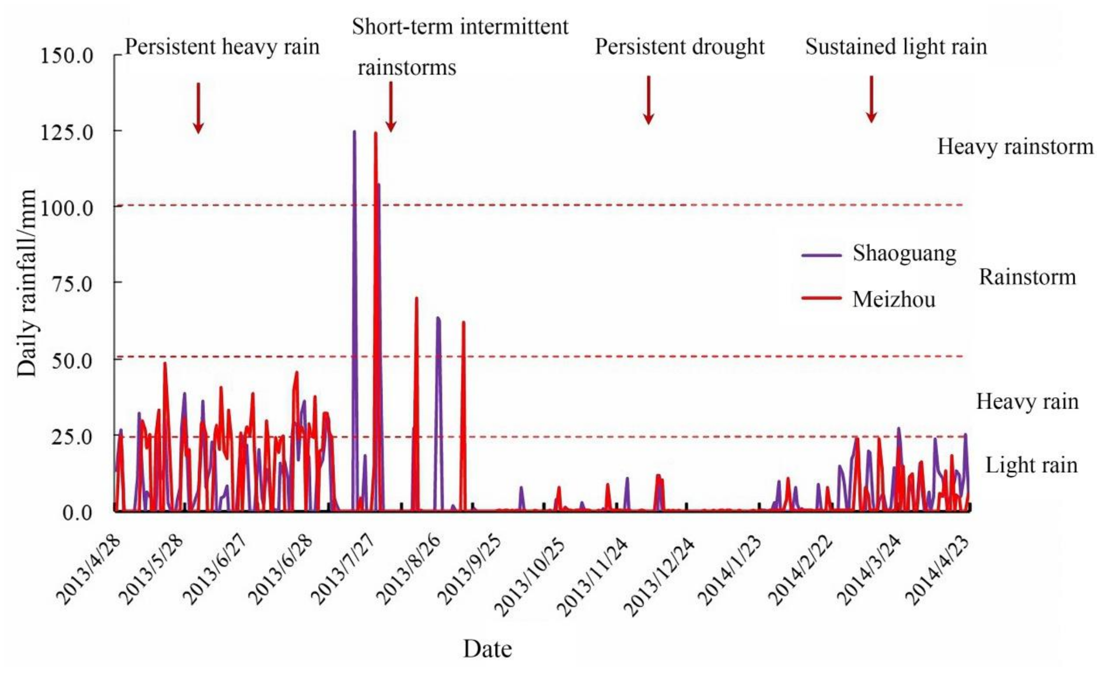


(**b**) Daily rainfall distribution map of Shaoguan-Heyaun

**Figure 15.** Rainfall in typical red-bed regions of Guangdong province.

The statistics show that the landslide pattern in the red beds of South China is governed by factors such as the rock mass structure, the slope height, and the height difference between the landslide niche and foot [53]. According to Cruden and Varnes' landslide classification, landslides fall into two groups: translational landslide and rotational landslide [54]. Global translational landslides are characterized by the failure mode of translational slides, and tractive landslides follow the mode of rotational slides.

(2) Failure mode

A global translational landslide occurs in nearly horizontal/slightly inclined layered slopes, especially in slopes containing thick hard rock mass with a thin weak rock mass interlayer (see Figure 16 and soft–hard interbedded rock mass structure in Table 1). When a slope is subjected to toe erosion and artificial cutting, the support in the front edge is weakened, and failure occurs along weak layers and structural planes. With the development of weathered fractures, the shear strength is expected to decrease because of rainfall infiltration. The thick rock mass layer will slide along the weak structural plane to the free face of the slope. During the sliding process, the relative positions between the different rock blocks remain almost unchanged, and the sliding surface is straight. The volume of the sliding part is approximately 3800–7000 $m^3$, and this type of slope failure usually leads to catastrophic landslides [55].

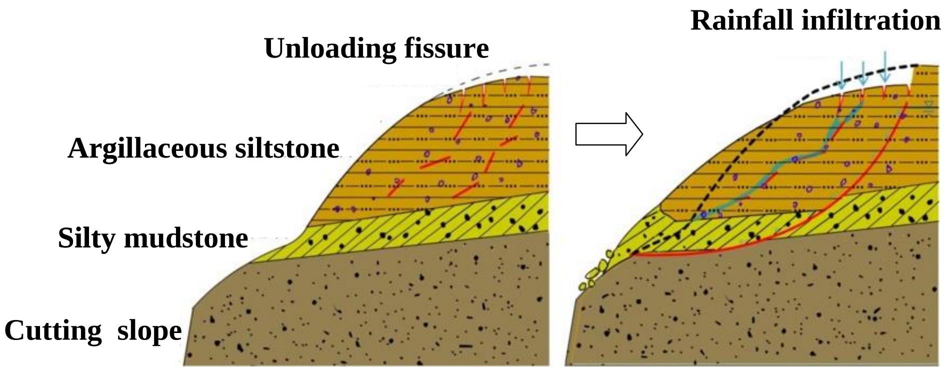


**Figure 16.** Schematic description of a global translational landslide in a red-bed slope in South China.

The tractive landslide accounts for over 50% of landslide events in the red beds in South China, with the average sliding volume ranging from 600 to 3500 $m^3$. These landslides are considered small-to-medium-scale landslides. Tractive landslides are initiated by a reduction in the shear strength of rock mass because of the water wash from rainfalls in the red-bed zone, leading to loss of support from the front edge [56]. In this context, the sliding force cannot be counterbalanced by the shear resistance from the rock mass itself. As shown in Figure 17, the rock mass slides step by step from front to back. The surface of rupture is curved concavely upward, and the slide movement is roughly rotational. The height difference between the front and back edges is approximately 10–55 m, and the largest thickness varies from 10 to 22.5 m. In addition, tension cracks usually develop at the back of the slope. With increasing excavation depth, the sliding interface develops from the superficial zone to the inner zone.

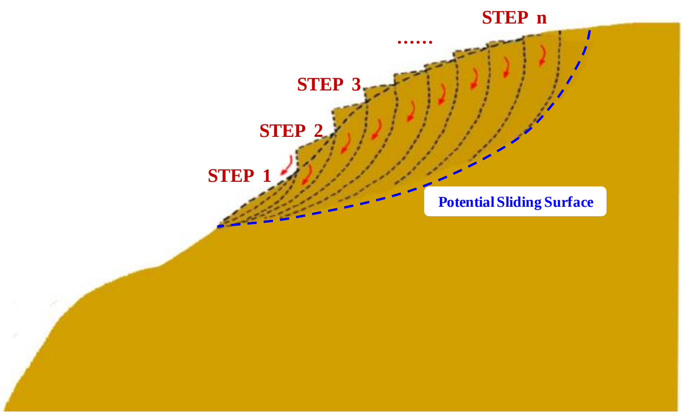


**Figure 17.** Schematic description of the progress of rotational landslides on red-bed slopes in South China.

Using rainfall data for the investigated area, model tests (Figure 18) were carried out to simulate the landslides of three slopes in this rainfall mode, and the results were in good agreement with the actual situation. In Figure 19a, a slope with a thick-layered soft–weak rock mass structure collapses near the foot of the slope, and the upper part of the free surface loses its support, which leads to a tractive landslide. A slope with a thick-layered hard rock mass structure with soft–weak rock mass is shown in Figure 19b. The soft–weak rock mass succumbs to the effects of rain softening and loses its strength, and an empty surface appears above the weak interbedded rock mass. The hard rock mass above the weak interbedded rock mass loses its support, which leads to a landslide. A soft–hard interbedded rock mass structure is shown in Figure 19c. There are many structural planes of weak rock mass in the upper part of the slope, and the sliding range is concentrated near the structural plane of the upper weak interlayer. The upper weak interlayer is located between the first and second grades of the slope.

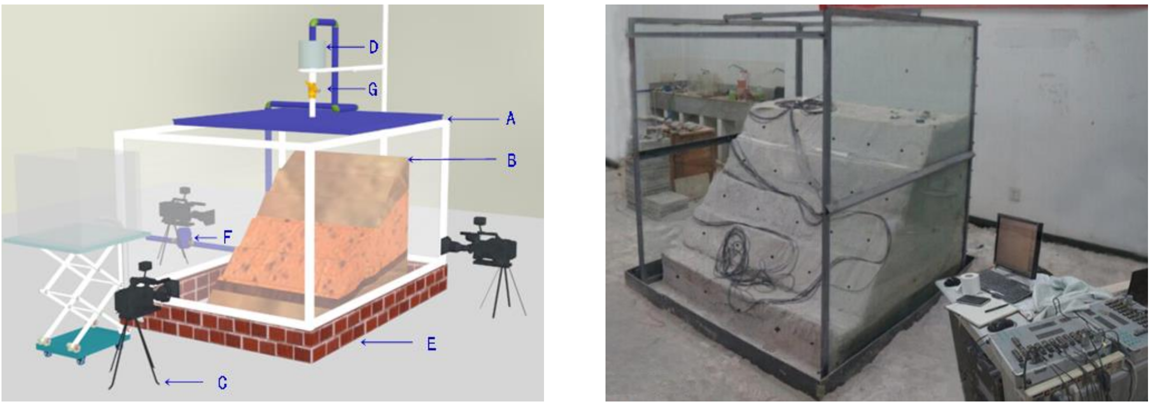


**(a)** Diagrammatic sketch **(b)** Physical photograph

**Figure 18.** Slope model test monitoring system (A. Transparent observation box. B. Test slope. C. High-resolution camera. D. Rainfall device. E. Water storage and groundwater level control device. F. Rainfall measuring device. G. Valve.).


(**a**) (**b**) (**c**)

**Figure 19.** Simulated slope failure modes: (**a**) slope with thick-layered soft-weak rock mass structure. (**b**) Thick-layered hard rock mass structure with soft-weak rock mass. (**c**) Soft-hard inter-bedded rock mass structure.

### 4.1.4. Toppling

Toppling is the phenomenon in which a hard rock mass topples to the free face about a certain point at the bottom in response to unloading and rebounding or when subjected to the actions of gravity and forces exerted by adjacent units or by fluids. If the dumping amplitude is adequately large, then it may collapse under the moment of gravity, and this might even lead to a deep sliding failure at the base [2,45,48].

Toppling in the red beds in South China usually occurs in thick hard rock slopes or in slopes with weak rock mass interlayers (see Table 1), which mostly consist of fractured stratum, weak clayey rock, mud intercalation, and so on. Steep wedge-shaped tension cracks develop at the top of a hard rock slope. As shown in Figure 20, these cracks are wide at the top but narrow at the bottom. According to the statistics, the width of such cracks, which are filled with loose soil, generally varies from 6 to 12 cm and can reach a maximum value of about 16 cm [41]. With the tension cracks developing vertically, the rock mass is gradually cut into strips or blocks, toppling around a certain point at the bottom of the rock mass (thick hard rock mass with weak rock interlayers topples at the contact between hard and soft rocks) under the effect of gravity.

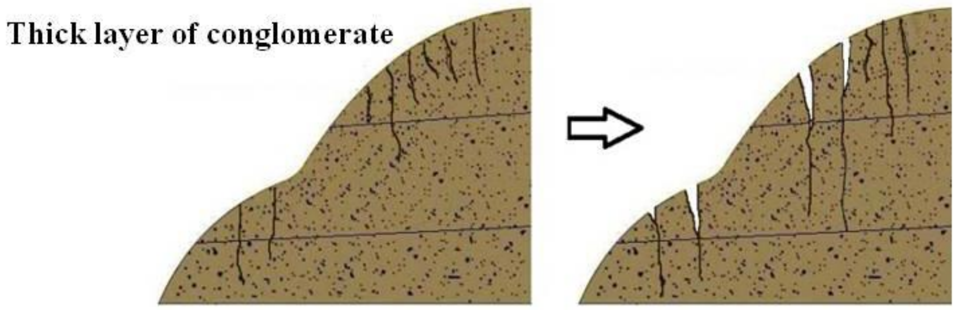


**Figure 20.** Schematic description of the tension crack destruction in red-bed slopes in South China.

(2) Failure mode

Slopes composed of a sandy conglomerate at the edge of the red-bed basin in South China are cut by orthogonal joints, along which weathering and erosion develop, making slopes deform on the side of the free face. It is generally observed that one group of steep structural planes is dragged apart, causing wedge-shaped tension cracks. With increasing depth and width of the tension cracks, rock mass units rotate forward about some pivotal point, which is low or below the unit.

For thick hard rock mass slopes containing weak rock interlayers (like the thick-layered hard rock mass structure with soft–weak rock mass in Table 1), differential deformation between hard and weak rock masses causes tension cracks in the upper sandy conglomerate to develop until toppling deformation appears. Furthermore, the weak strata are extruded through plastic flow under the weight of the upper hard rock mass and the actions of gravity and forces exerted by adjacent units or by fluids in the cracks. Recessed cavities are correspondingly created in the weak strata. Hence, the support of the upper hard rock mass becomes ineffective, causing tension cracks to develop and the slope to be toppled. This destruction tends to cause a large-scale landslide at the base. The volume of a landslide can be over one million cubic meters.

## 5. Conclusions

This paper discusses the geological background of the formation of the red beds in South China and analyzes as well as summarizes the features of the structural planes and the morphologies of the red-beds in the north of Guangdong Province. The structures of the rock mass in the red-bed areas in South China were classified on the basis of soft rock slope engineering features of the red beds along more than 10 highway projects in South China. The features of the geological hazards in the red-bed slopes possessing different structures were investigated, and typical failure modes in the red beds in South China were identified. The main findings are summarized as follows:

(1) The red beds in South China formed mainly through deposition under high-temperature and dry tropical–subtropical conditions. The sedimentation layers are cross-cut by fractures in the NE, NNE, and east–west (EW) directions. The red-bed basins formed along faults are generally randomly scattered in a small-to-medium-sized (hundreds of square kilometers on average) elongated area. Because of the influence of the sedimentation environment, the red beds in South China are mainly

interbedded in unequal thick and dip angles below 30°. In particular, the quaternary overburden layer usually exists in the red beds in South China.

(2) The structural planes of rock mass in the red beds in South China include primary weak stratification, a weak intercalation layer generated during sedimentation, and a tectonic weak cross-cutting plane created during tectonic movement. These planes also include a mudded intercalation layer created by the wet–dry cycling of the primary and tectonic weak interlayers. According to the characteristics of the structural planes and their morphologies, the rock mass in the red beds in South China are categorized into four types: (a) thick hard rock mass structures, (b) thick hard rock mass structure with weak intercalations, (c) thick soft rock mass structures, and (d) hard–soft interbedded rock mass structures.

(3) On the basis of the different rock mass structures in the red-bed soft rock areas in South China, four slope failure modes were identified: (a) weathering spalling and scouring, (b) rock falls, (c) landslides, and (d) tensile dumping. Weathering spalling and scouring occur frequently, and the other main types of geological hazards include rock falls, landslides, and tensile dumping.

**Author Contributions:** Conceptualization, C.Z., X.Y. and Z.L.; methodology, C.Z., X.Y. and Z.L.; software, Z.Y. and Y.L.; validation, C.Z., X.Y., Y.L. and Z.L.; formal analysis, C.Z., X.Y. and Z.L.; investigation, X.Y. and Y.L.; resources, C.Z. and Z.L.; data curation, X.Y. and Y.L.; writing—original draft preparation, X.Y., Y.L., Z.D., W.H. and W.M.; writing—review and editing, C.Z., X.Y., Y.L., Z.D., Z.L., W.H. and W.M.; visualization, C.Z., X.Y. and Z.L.; supervision, C.Z. and Z.L.; project administration, C.Z. and Z.L.; funding acquisition, C.Z. and Z.L.

**Funding:** The research was supported by the National Natural Science Foundation of China (NSFC) (Grant No. 41530638), the Special Fund Key Project of Applied Science and Technology Research and Development in Guangdong (No. 2015B090925016), the Special Support Plan for High-Level Talents of Guangdong Province (No. 2015TQ01Z344), the Science and Technology Program of Guangzhou, China (No. 201803030005).

**Conflicts of Interest:** The authors declare no conflict of interest.

## References

1. Peng, H.; Wu, Z.C. A Preliminary Study on the characteristics and the distribution of red beds. *Acta Sci. Nat. Univ. Sun Yat-Sen* **2003**, *42*, 109–113.
2. Liu, X.M. Research on Slaking Properties of Red Beds Soft Rock and Dynamic Deformation Properties of Embankment. Ph.D. Thesis, Hunan University, Changsha, China, 2006.
3. Yin, Y.P. Recent catastrophic landslides and mitigation in China. *J. Rock Mech. Geotech. Eng.* **2011**, *3*, 10–18. [CrossRef]
4. Cheng, Q.; Kou, X.B.; Huang, S.B.; Zhou, Y.J. The distributes and geologic environment characteristics of red beds in China. *J. Eng. Geol.* **2014**, *12*, 34–40.
5. Yin, Y.P.; Huang, B.L.; Wang, W.P.; Wei, Y.J.; Ma, X.H.; Ma, F.; Zhao, C.J. Reservoir-induced landslides and risk control in Three Gorges Project on Yangtze River, China. *J. Rock Mech. Geotech. Eng.* **2016**, *8*, 577–595. [CrossRef]
6. Wang, J.; Cao, Y.; Liu, K.; Costanzo, A.; Feely, M. Diagenesis and evolution of the lower Eocene red-bed sandstone reservoirs in the Dongying Depression, China. *Mar. Pet. Geol.* **2018**, *94*, 230–245. [CrossRef]
7. Hu, Q.J.; Huang, C.; Cai, Q.J. Multiple-factor analysis of fluid structure interaction about the stability of red bed mudstone slope. *Electron.-J. Geotech. Eng.* **2014**, *19G*, 1421–1432.
8. Zhou, Y.H.; Zhou, C.Y.; Liu, Z.; Yang, X.; Su, D.L.; Du, Z.C.; Liu, W. Model test for red-bed rock slope with weak intercalation affected by rainfall and its instability catastrophe model. *Electron.-J. Geotech. Eng.* **2016**, *21*, 3887–3903.
9. Allan, P. The weathering rates of some sand stone cliffs central weald. *Earth Surf. Process Landf.* **1991**, *16*, 83–91.
10. Robert, Y.; Ann, Y. *Sandstone Landform*; Springer: Berlin/Heidelberg, Germany, 1992; pp. 1–122.
11. Turkingtong, A.V.; Paradise, T.R. Sandstone weathering: A century of research and innovation. *Geomorphology* **2005**, *67*, 229–253.
12. Warke, P.A.; Mckinley, J.; Smith, B.J. Variable weathering response in sandstone: Factors controlling decay sequences. *Earth Surf. Process Landf.* **2006**, *31*, 715–735. [CrossRef]
13. Handrij, H.; Václav, C.; Andrew, J. *Sandstone Landscapes*; Nakladatelství Academic: Praha, Czech Republic, 2007; pp. 12–125.

14. Gu, D.Z. *Rock Engineering Geological Mechanics Foundation*; Science Press: Beijing, China, 1979.
15. Ju, H.Y.; Gu, R.J. Geologic feature and engineering geological problems of red beds in South China. *Shanghai Geol.* **1983**, *3*, 1–16.
16. Sun, G.Z. On the theory of structure-controlled rockmass. *J. Eng.* **1993**, *1*, 14–18.
17. Troalen, J.P. Ultrastructural approach to the behaviour of geomaterials: Clayey geomaterials. *Bull. Int. Assoc. Eng. Geol.* **1994**, *4*, 73–83. [CrossRef]
18. Hillier, R.D.; Williams, B.P.J. Sedimentation and tectonies: The marine Siluria-basal lower Old Red Sandstone transition in southwest Wales. *Geol. J.* **2004**, *39*, 237–256. [CrossRef]
19. Hu, H.T.; Zhao, X.Y. Studies on rockmass structure in slope of red bed in China. *Geotech. Eng.* **2006**, *28*, 689–694.
20. Zhou, C.Y.; Zhu, F.X.; Zheng, L. Research on saturation test and softening critical phenomena of soft rocks. *Rock Soil Mech.* **2010**, *31*, 1709–1715.
21. Zhou, C.Y.; Zhu, F.X. An elasto-plastic damage constitutive model with double yield surfaces for saturated soft rock. *Int. J. Rock Mech. Min. Sci.* **2010**, *47*, 385–395. [CrossRef]
22. Yamashita, I.; Surinkum, A.; Wada, Y.; Fujihara, M.; Yokoyama, M.; Zaman, H.; Otofuji, Y. Paleomagnetism of the Middle-Late Jurassic to Cretaceous red beds from the Peninsular Thailand: Implications for collision tectonic. *J. Asian Earth Sci.* **2011**, *40*, 784–796. [CrossRef]
23. Yang, Z.F.; Yue, Z.Q.; Li, L.H. Design, construction and mechanical behavior of relics of complete large Longyou rock caverns carved in argillaceous siltstone ground. *J. Rock Mech. Geotech. Eng.* **2011**, *3*, 131–152. [CrossRef]
24. Li, X.; Tan, R. Superficial Deformation and Failure Modes of Small and Medium Scale Slopes in Red Bed Sichuan Basin. In Proceedings of the 3rd International Conference on Transportation Engineering, Chengdu, China, 23–25 July 2011; pp. 2050–2055.
25. Lu, H.F.; Liu, Q.S.; Chen, C.X.; Wu, Y.X.; Li, J.L. Experimental study on mechanical characteristic of weak interlayer in red-bed soft rock slope. *Energy Educ. Sci. Technol. Part A Energy Sci. Res.* **2012**, *30*, 467–474.
26. Chen, J.; Dai, F.C.; Xu, L.; Chen, S.; Wang, P.F.; Long, W.; Shen, N.Q. Properties and microstructure of a natural slip zone in loose deposits of red beds, southwestern China. *Eng. Geol.* **2014**, *183*, 53–64. [CrossRef]
27. Akintunde, O.M.; Knapp, C.C.; Knapp, J.H. Tectonic significance of porosity and permeability regimes in the red beds formations of the South Georgia Rift Basin. *Tectonophysics* **2014**, *632*, 1–7. [CrossRef]
28. Gao, Q.; Zhang, Q.Y.; Zhang, X.T.; Zhang, L.Y. Geomechanical Model Test and Energy Mechanism Analysis of Zonal Disintegration in Deep Surrounding Rock. *Geosciences* **2018**, *8*, 237. [CrossRef]
29. Zhang, Z.Y.; Wang, S.T.; Wang, L.S. *Engineering Geological Analysis Principle*; Geological Publishing House: Beijing, China, 1994.
30. GB50021. *Code for Geotechnical Engineering Investigation*; China Building Industry Press: Beijing, China, 2001.
31. Li, Z.Y.; Zou, J.R.; Xie, Q. Studies on engineering geologic and systematic clustering on roadcuts and slopes in red beds. *Geotech. Investig. Surv.* **2002**, *2*, 5–7.
32. Chi, E.A.; Tao, T.J.; Zhao, M.S.; Kang, Q. Failure Mode Analysis of Bedding Rock Slope Affected by Rock Mass Structural Plane. *Appl. Mech. Mater.* **2014**, *602–605*, 594–597. [CrossRef]
33. Sun, S.R.; Sun, H.Y.; Wang, Y.J.; Wei, J.H.; Liu, J.; Kanungo, D.P. Effect of the combination characteristics of rock structural plane on the stability of a rock-mass slope. *Bull. Eng. Geol. Environ.* **2014**, *73*, 987–995. [CrossRef]
34. Zhong, W.; Tan, Z.Y.; Qiao, L. Stability Analysis of Rock Slope Based on Preferred Structural Plane. *Adv. Mater. Res.* **2011**, *243–249*, 2254–2258. [CrossRef]
35. Guo, Y.C.; Xie, Q.; Wen, J.Q. Engineering criterion of structure-stability of soft rocks of redbeds. *Hydrogeol. Eng. Geol.* **2010**, *6*, 86–90.
36. Cheng, C.; Zhou, A.G.; Zhou, J.W. Landscape characteristics and causes process of Danxia landforms in Baishishan of Guiping city, Guangxi Province. *Earth Sci. J. China Univ. Geosci.* **2013**, *38*, 641–648.
37. Li, X.; He, Q.C.; Dong, Y.; Cao, X.J.; Wang, Z.Y.; Duan, X.M. An analysis of characteristics and evolution of Danxia Landform in the south of Chishui County, Guizhou. *Acta Geosci. Sin.* **2013**, *34*, 501–508.
38. Su, T.M.; Zhang, Y.G.; Zhang, T.Z.; Liu, Y.L. Rock falls in horizontal strata due to differential weathering. *Eng. Geol. Soc. Territ.* **2015**, *2*, 1745–1751.
39. Dong, J.Y.; Yang, J.H.; Wu, F.Q.; Wang, D.; Yang, G.X. Research on collapse of high cutting slope with horizontal soft-hard alternant strata in Three Gorges reservoir area. *Rock Soil Mech.* **2010**, *31*, 151–157.

40. Lin, Z.Y. *Geotechnical Engineering Reconnaissance and Design Manual*; Liaoning Science and Technology Press: Shenyang, China, 1996.
41. Yang, X. Study on the environment effect model of the red-bed soft rock slope. Ph.D. Thesis, Sun Yat-sen University, Guangzhou, China, 2015.
42. Andrew, S.G.; Heather, A.V. The nature and pattern of debris liberation by salt weathering: A laboratory study. *Earth Surf. Process Landf.* **1995**, *20*, 437–449.
43. Kevin, H.; Alida, H. Weathering by wetting and drying: Some experimental results. *Earth Surf. Process Landf.* **1996**, *21*, 365–376.
44. Phillips, J.D.; Luckow, K.; Marion, D.A.; Adams, K.R. Rock fragment distributions and regolith evolution in the Ouachita mountains, Arkansas, USA. *Earth Surf. Process Landf.* **2005**, *30*, 429–442. [CrossRef]
45. Niemann, W.L. Lessons learned from rates of mudrock undercutting measured over two time periods. *Environ. Eng. Geosci.* **2009**, *15*, 117–131. [CrossRef]
46. Chengdu Railway Bureau. *Plastering Prevent of Clay Rock Slope Weathering Flaking*; 1963 Railway Science and technology papers report anthology the 11 series (Engineering Geology and Roadbed Engineering); China Railway Press: Beijing, China, 1965.
47. Yang, Z.C.; Zhang, J.Y.; Zhou, D.P. Study on fast weathering characteristics of red bed mudstone slope. *J. Rock Mech. Eng.* **2006**, *25*, 275–283.
48. Pritchard, M.A.; Savigny, K.W. Heather Hill landslide: An example of a large scale toppling failure. *Can. Geotech. J.* **1989**, *26*, 737–742.
49. Phien-Wej, N.; Nutalaya, P.; Aung, Z.; Tang, Z.B. Catastrophic landslides and debris flows in Thailand. *Bull. Int. Assoc. Eng. Geol.* **1993**, *48*, 93–100. [CrossRef]
50. Zheng, Y.R.; Chen, Z.Y.; Wang, G.X.; Ling, T.Q. *Slope and Landslide Management*; People's Communication Press: Beijing, China, 2010.
51. Xu, W.Y.; Zhang, Q.; Zhang, J.C.; Wang, R.B.; Wang, R.K. Deformation and control engineering related to huge landslide on left bank of Xiluodu reservoir, South-West China. *Eur. J. Environ. Civ. Eng.* **2013**, *17* (Suppl. 1), 249–268. [CrossRef]
52. Zhang, M.; Yin, Y.P.; Huang, B.L. Mechanisms of rainfall-induced landslides in gently inclined red beds in the eastern Sichuan Basin, SW China. *Landslides* **2015**, *12*, 973–983. [CrossRef]
53. Gong, Q.H. DEM and GIS based analysis of topographic and geomorphologic factors of shallow landslide in red soil hilly region of South China. *Int. J. Earth Sci. Eng.* **2014**, *7*, 393–399.
54. Cruden, D.M.; Varnes, D.J. *Landslide types and processes. InLandslides: Investigation and Mitigation*; Turner, A.K., Shuster, R.L., Eds.; Transp Res Board, Spec Rep 247; National Academy Press: Washington, DC, USA, 1996; pp. 36–75.
55. Tang, M.G.; Xu, Q.; Huang, X.B.; Xu, K.X.; Cheng, W.M.; Wang, K. Recognition and Genetic Mechanism of Sanmashan Deep-Seated Landslide, Three Gorges Reservoir Area, China. *Eng. Geol. Soc. Territ.* **2015**, *2*, 587–591.
56. Zhang, S.; Xu, Q.; Hu, Z. Effects of rainwater softening on red mudstone of deep-seated landslide, Southwest China. *Eng. Geol.* **2016**, *204*, 1–13. [CrossRef]